The effect of surface roughness on the adhesion of elastic solids — **Source link**

Bo N. J. Persson, Erio Tosatti

Institutions: Forschungszentrum Jülich

Related papers:

- Surface energy and the contact of elastic solids

- Contact of Nominally Flat Surfaces

- Effect of contact deformations on the adhesion of particles

- Theory of rubber friction and contact mechanics

- Contact between rough surfaces and a criterion for macroscopic adhesion.

The effect of surface roughness on the adhesion of elastic solids

B. N. J. Persson[a)]

*IFF, FZ-Jülich, 52425 Jülich, Germany and International School for Advanced Studies (SISSA),
Via Beirut 2-4, I-34014, Trieste, Italy*

E. Tosatti

*International School for Advanced Studies (SISSA), Via Beirut 2-4, I-34014, Trieste, Italy, INFM,
Unita' SISSA, Trieste, Italy, and International Centre for Theoretical Physics, P.O. Box 586, I-34014,
Trieste, Italy*

We study the influence of surface roughness on the adhesion of elastic solids. Most real surfaces have roughness on many different length scales, and this fact is taken into account in our analysis. We consider in detail the case when the surface roughness can be described as a self-affine fractal, and show that when the fractal dimension $D_f > 2.5$, the adhesion force may vanish, or be at least strongly reduced. We consider the block-substrate pull-off force as a function of roughness, and find a partial detachment transition preceding a full detachment one. The theory is in good qualitative agreement with experimental data. © *2001 American Institute of Physics.*
[DOI: 10.1063/1.1398300]

I. INTRODUCTION

Even a highly polished surface has surface roughness on many different length scales. When two bodies with nominally flat surfaces are brought into contact, the area of real contact will usually only be a small fraction of the nominal contact area. We can visualize the contact regions as small areas where asperities from one solid are squeezed against asperities of the other solid; depending on the conditions the asperities may deform elastically or plastically.

How large is the area of *real* contact between a solid block and the substrate? This fundamental question has extremely important practical implications. For example, it determines the contact resistivity and the heat transfer between the solids. It is also of direct importance for sliding friction,[1] e.g., the rubber friction between a tire and a road surface, and it has a major influence on the adhesive force between two solid blocks in direct contact. One of us has developed a theory of contact mechanics,[2] valid for randomly rough (e.g., self-affine fractal) surfaces, but neglecting adhesion. Adhesion is particularly important for elastically soft solids, e.g., rubber or gelatine, where it may pull the two solids in direct contact over the whole nominal contact area.

In this paper we discuss adhesion for randomly rough surfaces. We first calculate the block-substrate pull-off force under the assumption that there is complete contact in the nominal contact area. We assume that the substrate surface has roughness on many different length scales, and consider in detail the case where the surfaces are self-affine fractal. We also study pull-off when only partial contact occurs in the nominal contact area.

The influence of surface roughness on the adhesion between rubber (or any other elastic solid) and a hard substrate has been studied in a classic paper by Fuller and Tabor.[3]

They found that already a relative small surface roughness can completely remove the adhesion. In order to understand the experimental data they developed a very simple model based on the assumption of surface roughness on a single length scale. In this model the rough surface is modeled by asperities all of the same radius of curvature and with heights following a Gaussian distribution. The overall contact force was obtained by applying the contact theory of Johnson, Kendall, and Roberts[4] (JKR) to each individual asperity. The theory predicts that the pull-off force, expressed as a fraction of the maximum value, depends upon a single parameter, which may be regarded as representing the statistically averaged competition between the compressive forces exerted by the higher asperities trying to pry the surfaces apart and the adhesive forces between the lower asperities trying to hold the surfaces together. We believe that this picture of adhesion developed by Tabor and Fuller would be correct *if* the surfaces had roughness on a single length scale as assumed in their study. However, when roughness occurs on many different length scales, a qualitatively new picture emerges (see the following), where, e.g., the adhesion force may even vanish (or at least be strongly reduced), if the rough surface can be described as a self-affine fractal with fractal dimension $D_f > 2.5$. We also note that the formalism used by Fuller and Tabor is only valid at "high" surface roughness, where the area of real contact (and the adhesion force) is very small. The present theory, on the other hand, is particularly accurate for "small" surface roughness, where the area of real contact equals the nominal contact area.

II. QUALITATIVE DISCUSSION

Assume that a uniform stress σ acts within a circular area (radius R) centered at a point P on the surface of a semi-infinite elastic body with elastic modulus E, see Fig. 1. This will give rise to a perpendicular displacement u of P by

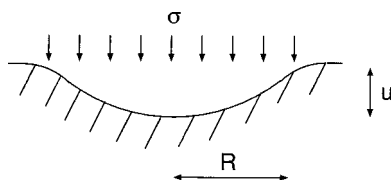[a)]Electronic mail: b.persson@fz-juelich.de

FIG. 1. A uniform stress σ, acting within a circular area (radius R) on the surface of a semi-infinite elastic medium, gives rise to a displacement u.

FIG. 2. The adhesion interaction pulls the rubber into complete contact with the rough substrate surface.

a distance which is easy to calculate using continuum mechanics: $u/R \approx \sigma/E$. This result can also be derived from simple dimensional arguments. First, note that u must be proportional to σ since the displacement field is linearly related to the stress field. However, the only other quantity in the problem with the same dimension as the stress σ is the elastic modulus E so u must be proportional to σ/E. Since R is in turn the only quantity with the dimension of length we get at once $u \sim (\sigma/E)R$. Thus, if h and λ represent perpendicular and parallel roughness length scales, respectively, then if $h/\lambda \approx \sigma/E$, the perpendicular pressure σ will be just large enough to deform the rubber to make contact with the substrate everywhere.

Let us now consider the role of the rubber–substrate adhesion interaction. When the rubber deforms and fills out a surface cavity of the substrate, an elastic energy $U_{el} \approx E\lambda h^2$ will be stored in the rubber. Now, if this elastic energy is smaller than the gain in adhesion energy $U_{ad} \approx -\Delta\gamma\lambda^2$, where $-\Delta\gamma$ is the local change of surface free energy upon contact due to the rubber–substrate interaction (which usually is mainly of the van der Waals type), then (even in the absence of the load F_N) the rubber will deform *spontaneously* to fill out the substrate cavities. The condition $U_{el} = -U_{ad}$ gives $h/\lambda \approx (\Delta\gamma/E\lambda)^{1/2}$. For example, for very rough surfaces with $h/\lambda \approx 1$, and with parameters typical of rubber $E = 1$ MPa and $\Delta\gamma = 3$ meV/Å^2, the adhesion interaction will be able to deform the rubber and completely fill out the cavities if $\lambda < 0.1$ μm. For very smooth surfaces $h/\lambda \sim 0.01$ or smaller, so that the rubber will be able to follow the surface roughness profile up to the length scale $\lambda \sim 1$ mm or longer.

The above-mentioned discussion assumes roughness on a single length scale λ. But the surfaces or real solids have roughness on a wide distribution of length scales. Assume, for example, a self-affine fractal surface. In this case the statistical properties of the surface are invariant under the transformation

$$\mathbf{x} \rightarrow \mathbf{x}\zeta, \quad z \rightarrow z\zeta^H,$$

where $\mathbf{x} = (x,y)$ is the two-dimensional position vector in the surface plane, and where $0 < H < 1$. This implies that if h_a is the amplitude of the surface roughness on the length scale λ_a, then the amplitude h of the surface roughness on the length scale λ will be of order

$$h \approx h_a(\lambda/\lambda_a)^H.$$

A necessary condition for adhesional-induced complete contact on the length scale λ is that $E_{ad} > E_{el}$, i.e., $\Delta\gamma\lambda > Eh^2$, which gives
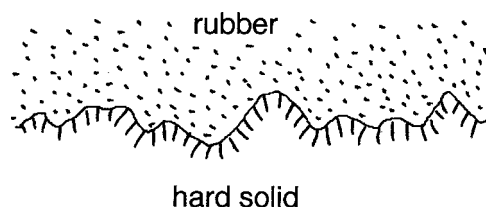
$$\Delta\gamma\lambda > Eh_a^2 \left(\frac{\lambda}{\lambda_a} \right)^{2H}$$

or

$$\left(\frac{\lambda}{\lambda_a} \right)^{2H-1} < \frac{\Delta\gamma\lambda_a}{Eh_a^2}. \tag{1}$$

Assume first that $H > 1/2$. In this case, if $\lambda_a < \lambda$ we get $(\lambda/\lambda_a)^{2H-1} > 1$, and condition (1) gives $\Delta\gamma\lambda_a/Eh_a^2 > 1$. Thus, adhesion will be important on any length scale $\lambda_a < \lambda$. In particular, if λ is the long-distance cutoff length λ_0 in the self-affine fractal distribution, then *complete contact will occur at the interface*. More generally, if $\lambda = Eh^2/\Delta\gamma < \lambda_0$, the contact consists of a set of disconnected contact regions of linear size λ; in each such region perfect contact occurs.

Consider now instead $H < 1/2$. In this case, if $\lambda_a < \lambda$ we get $(\lambda/\lambda_a)^{2H-1} < 1$, and condition (1) no longer guarantees that $\Delta\gamma\lambda_a/Eh_a^2 > 1$. In fact, it is easy to show that at short enough length scale λ_a, $\Delta\gamma\lambda_a/Eh_a^2 < 1$. Thus, without a short-distance cutoff, *adhesion and the area of real contact will vanish*. Hence, in spite of the fact that the contact at first may seems to be perfect on large scales (since $\Delta\gamma\lambda > Eh^2$), there is, in fact, no contact at all since $\Delta\gamma\lambda_a < Eh_a^2$ holds at short enough length scale λ_a. In reality, a finite short-distance cutoff will always occur, but this case requires a more detailed study (see Sec. III). Also, in the above-mentioned analysis we have neglected that the area of real contact depends on h (i.e., it is of order λ^2 only when $h/\lambda \ll 1$). A more accurate analysis follows.

III. INTERFACIAL ELASTIC AND ADHESION ENERGIES FOR ROUGH SURFACES

Assume that a flat rubber surface is in contact with the rough surface of a hard solid. Assume that because of the rubber–substrate adhesion interaction, the rubber deforms elastically and makes contact with the substrate everywhere, see Fig. 2.

Let us calculate the difference in free energy between the rubber block in contact with the substrate and the noncontact case. Let $z = h(\mathbf{x})$ denote the height of the rough surface above a flat reference plane (chosen so that $\langle h \rangle = 0$). Assume first that the rubber is in direct contact with the substrate over the whole nominal contact area. The surface adhesion energy is assumed proportional to the contact area so that

$$U_{ad} = -\Delta\gamma \int d^2x [1 + (\nabla h(\mathbf{x}))^2]^{1/2}$$

$$\approx -\Delta\gamma\left[A_0 + \frac{1}{2}\int d^2x(\nabla h)^2\right], \qquad (2)$$

where we have assumed $|\nabla h| \ll 1$. Now, using

$$h(\mathbf{x}) = \int d^2q\, h(\mathbf{q})e^{i\mathbf{q}\cdot\mathbf{x}}$$

we get

$$\int d^2x(\nabla h)^2 = \int d^2x \int d^2q\, d^2q'(-\mathbf{q}\cdot\mathbf{q}')$$

$$\times \langle h(\mathbf{q})h(\mathbf{q}')\rangle\, e^{i(\mathbf{q}+\mathbf{q}')\cdot\mathbf{x}}$$

$$= (2\pi)^2\int d^2q\, q^2\langle h(\mathbf{q})h(-\mathbf{q})\rangle$$

$$= A_0\int d^2q\, q^2C(q), \qquad (3)$$

where the surface roughness power spectrum is

$$C(q) = \frac{1}{(2\pi)^2}\int d^2x\langle h(\mathbf{x})h(\mathbf{0})\rangle e^{-i\mathbf{q}\cdot\mathbf{x}}, \qquad (4)$$

where $\langle\cdots\rangle$ stands for ensemble average. Thus, using Eqs. (2) and (3):

$$U_{ad}\approx -A_0\Delta\gamma\left[1 + \frac{1}{2}\int d^2q\, q^2C(q)\right]. \qquad (5)$$

Next, let us calculate the elastic energy stored in the deformation field in the vicinity of the interface. Let $u_z(\mathbf{x})$ be the normal displacement field of the surface of the elastic solid. We get

$$U_{el}\approx -\frac{1}{2}\int d^2x\langle u_z(\mathbf{x})\sigma_z(\mathbf{x})\rangle$$

$$= -\frac{(2\pi)^2}{2}\int d^2q\langle u_z(\mathbf{q})\sigma_z(-\mathbf{q})\rangle. \qquad (6)$$

Next, we know that[5]

$$u_z(\mathbf{q}) = M_{zz}(\mathbf{q})\sigma_z(\mathbf{q}), \qquad (7)$$

where

$$M_{zz}(\mathbf{q}) = -\frac{2(1-\nu^2)}{Eq}, \qquad (8)$$

E being the elastic modulus and ν the Poisson ratio. If we assume that complete contact occurs between the solids, then $u_z = h(\mathbf{x})$ and from Eqs. (4) and (6)–(8),

$$U_{el}\approx -\frac{(2\pi)^2}{2}\int d^2q\langle u_z(\mathbf{q})u_z(-\mathbf{q})\rangle[M_{zz}(-\mathbf{q})]^{-1}$$

$$= \frac{A_0E}{4(1-\nu^2)}\int d^2q\, qC(q). \qquad (9)$$

The change in the free energy when the rubber block moves in contact with the substrate is given by the sum of Eqs. (5) and (9):

$$U_{el} + U_{ad} = -\Delta\gamma_{eff}A_0,$$

where

$$\Delta\gamma_{eff} = \Delta\gamma\left[1 + \pi\int_{q_0}^{q_1}dq\, q^3C(q)\right.$$

$$\left. -\frac{\pi E}{2(1-\nu^2)\Delta\gamma}\int_{q_0}^{q_1}dq\, q^2C(q)\right]. \qquad (10)$$

The above-given theory is valid for surfaces with arbitrary random roughness, but will now be applied to self-affine fractal surfaces. It has been found that many "natural" surfaces, e.g., surfaces of many materials generated by fracture, can be approximately described as self-affine surfaces over a rather wide roughness size region. A self-affine fractal surface has the property that if we make a scale change that is appropriately different along the two directions, parallel and perpendicular, then the surface does not change its morphology.[6] Recent studies have shown that even asphalt road tracks (of interest for rubber friction) are (approximately) self-affine fractal, with an upper cutoff length $\lambda_0 = 2\pi/q_0$ of order of a few millimeters.[7] For a self affine fractal surface:[6,8] $C(q) = 0$ for $q < q_0$, while for $q > q_0$:

$$C(q) = \frac{H}{2\pi}\left(\frac{h_0}{q_0}\right)^2\left(\frac{q}{q_0}\right)^{-2(H+1)}, \qquad (11)$$

where $H = 3 - D_f$ (where the fractal dimension $2 < D_f < 3$), and where q_0 is the lower cutoff wave vector, and h_0 is determined by the rms roughness amplitude, $\langle h^2\rangle = h_0^2/2$. We note that $C(q)$ can be measured directly, using many different methods, e.g., using stylus instruments or optical instruments.[9]

Substituting Eq. (11) in Eq. (10) gives

$$\frac{\Delta\gamma_{eff}}{\Delta\gamma} = 1 + \frac{1}{2}(q_0h_0)^2g(H) - \frac{Eh_0^2q_0}{4(1-\nu^2)\Delta\gamma}f(H), \qquad (12)$$

where

$$f(H) = \frac{H}{1-2H}\left[\left(\frac{q_1}{q_0}\right)^{1-2H} - 1\right],$$

$$g(H) = \frac{H}{2(1-H)}\left[\left(\frac{q_1}{q_0}\right)^{2(1-H)} - 1\right].$$

If we introduce the length $\delta = 4(1-\nu^2)\Delta\gamma/E$, then Eq. (12) takes the form

$$\frac{\Delta\gamma_{eff}}{\Delta\gamma} = 1 + (q_0h_0)^2\left(\frac{1}{2}g(H) - \frac{1}{q_0\delta}f(H)\right). \qquad (13)$$

In Fig. 3 we show $f(H)$ and $g(H)$ as a function of H. Note that the present theory is valid only if $(q_0h_0)^2g(H)/2 < 1$, otherwise the expansion of the square-root function in Eq. (2) is invalid.

Let us emphasize that the present theory is strictly valid only for purely elastic solids; many real solids (e.g., most polymers)[10] behave in a viscoelastic manner, and in these cases $\Delta\gamma$ may be much larger than in the adiabatic limit, and the theory presented in this paper is no longer valid. Viscoelastic effects may be particularly important for rough surfaces, where, during pull off, the roughness introduces fluctuating forces with a wide distribution of frequencies. The same effect operates during sliding as described in a recent work on rubber friction.[11]
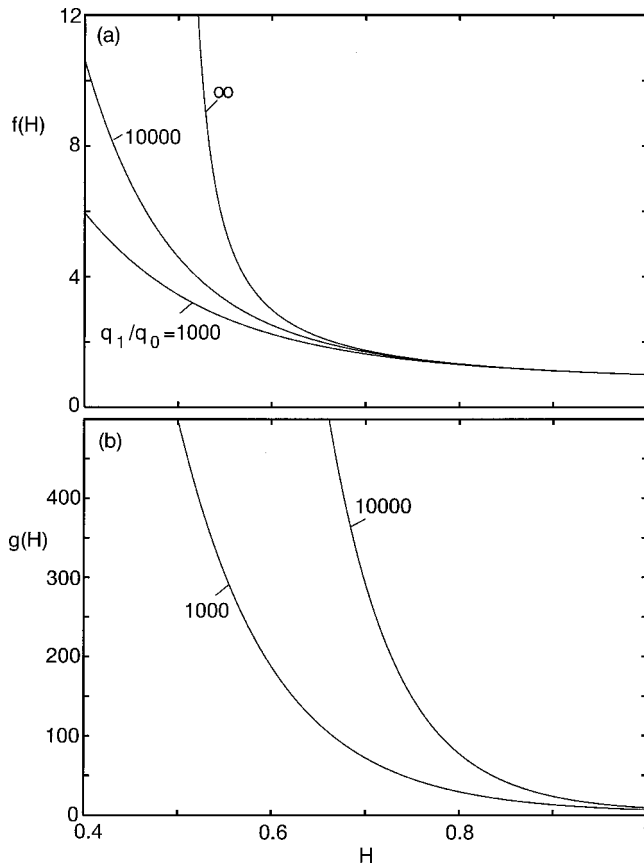
FIG. 3. The functions $f(H)$ and $g(H)$ are defined in the text.

Consider first an elastically very soft solid, e.g., jelly. In this case, using $E \approx 10^4$ Pa and $\Delta\gamma \approx 3$ meV/Å^2, we get $\delta \approx 10\,\mu$m, and since typically $q_0 = 2\pi/\lambda_0 \sim (10\,\mu\text{m})^{-1}$ and $g(H) \gg f(H)$, we expect $\Delta\gamma_{\text{eff}} > \Delta\gamma$. Thus, for an (elastically) very soft solid the adhesion force may increase upon roughening the substrate surface. This effect has been observed experimentally for rubber in contact with a hard, rough substrate,[12,13] and the present theory explains under exactly what conditions that will occur (see the following).

Note that if the condition $g(H)/2 > f(H)/(q_0\delta)$ is satisfied, the adhesion force (for small enough h_0) will increase with increasing amplitude h_0 of the surface roughness. We may define a critical elasticity E_c such that if $E < E_c$, $\Delta\gamma_{\text{eff}}$ increases with increasing h_0, while it decreases if $E > E_c$. E_c is determined by the condition $g(H)/2 = f(H)/(q_0\delta)$, which gives

$$E_c = 2(1-\nu^2)\Delta\gamma q_0 g(H)/f(H).$$

This expression for E_c depends on the nature of the surface roughness via the cutoff wave vector q_0 and the fractal exponent $H = 3 - D_f$. These quantities can be obtained from measurements of the surface roughness power spectra $C(q)$. Such measurements have not been performed for any of the systems for which the dependence of the adhesion on the roughness amplitude h_0 has been studied. However, measurements[9] of $C(q)$ for similar surfaces as those used in the adhesion experiments have shown that typically $H \approx 0.8$ and $\lambda_0 = 2\pi/q_0 \approx 100\,\mu$m. For $H \approx 0.8$, Fig. 3 gives $g(H)/f(H) \sim 100$ and with the measured (for rubber in con-

tact with most hard solids) $\Delta\gamma \approx 3$ meV/Å^2 we get $E_c \approx 1$ MPa. This is in very good agreement with experimental observations. Thus, Briggs and Briscoe[12] observed a strong roughness-induced increase in the pull-off force for rubber with the elastic modulus $E = 0.06$ MPa, but a negligible increase when $E = 0.5$ MPa. Similarly, Fuller and Roberts[13] observed an increase in the pull-off force for rubbers with $E = 0.4$, 0.14, and 0.07 MPa, but a continuous decrease for rubbers with $E = 1.5$ and 3.2 MPa. It would be extremely interesting to perform a detailed test of the theory for surfaces for which the surface roughness power spectra $C(q)$ has been measured.

According to Eq. (13), the roughness-induced contribution to $\Delta\gamma_{\text{eff}}$ scales as $\sim h_0^2$. This scaling is exact for the contribution from elastic deformations (as long as complete contact occurs), but is only valid for small enough h_0 for the adhesion contribution. For large h_0 the expansion in Eq. (2) is invalid, and one obtains instead

$$U_{\text{ad}} \approx -\Delta\gamma \int d^2x |\nabla h(\mathbf{x})|,$$

which varies linearly with h_0. Thus, for large enough h_0 the (negative) contribution to $\Delta\gamma_{\text{eff}}$ from the elastic deformations will always dominate, and this explains why the pull-off force always decreases for large enough h_0, even when the elastic modulus of the rubber is very small.[12,13] In fact, we can derive an expression for $\Delta\gamma_{\text{eff}}$ which is approximately valid also for large h_0, as follows: Let us write Eq. (2) as (see Appendix B for the derivation of the exact result)

$$U_{\text{ad}} = -\Delta\gamma A_0 \langle [1 + (\nabla h(\mathbf{x}))^2]^{1/2} \rangle$$
$$\approx -\Delta\gamma A_0 [1 + \langle (\nabla h(\mathbf{x}))^2 \rangle]^{1/2},$$

where

$$\langle (\nabla h(\mathbf{x}))^2 \rangle = \frac{1}{A_0} \int d^2x (\nabla h(\mathbf{x}))^2 = 2\pi \int_{q_0}^{q_1} dq\, q^3 C(q).$$

Thus, for a self-affine fractal surface Eq. (13) is replaced with

$$\frac{\Delta\gamma_{\text{eff}}}{\Delta\gamma} \approx [1 + (q_0 h_0)^2 g(H)]^{1/2} - (q_0 h_0)^2 \frac{1}{q_0\delta} f(H). \quad (14a)$$

If we denote $\xi = h_0 q_0 g^{1/2}$ then Eq. (14a) becomes

$$\frac{\Delta\gamma_{\text{eff}}}{\Delta\gamma} = (1 + \xi^2)^{1/2} - \frac{E}{2E_c}\xi^2. \quad (14b)$$

This function is shown in Fig. 4 for $E_c/E = 1$ and 2 (dashed lines). The solid lines in Fig. 4 are obtained using the exact result derived in Appendix B [see Eq. (B2)]. If we assume that the pull-off force is proportional to $\Delta\gamma_{\text{eff}}$ [as expected for a rubber ball, see Eq. (21)], we obtain the h_0 dependence of the pull-off force shown in Fig. 4, which is in good qualitative agreement with experiment.[13]

If it would be possible to prepare surfaces with different roughness amplitude h_0 but constant q_0 (and H), then it is easy to prove from Eq. (14b) that the maximum of $\Delta\gamma_{\text{eff}}$ as a function of h_0 is
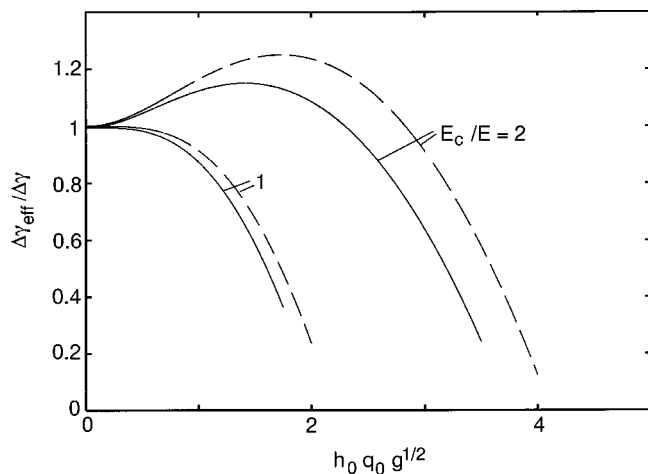
FIG. 4. The effective change in surface energy as a function of the dimensionless parameter $h_0 q_0 g^{1/2}$ for $E_c/E = 1$ and 2. The solid lines are obtained using the exact result given by Eq. (B2), while the dashed lines are obtained using the approximation (14b).

$$(\Delta\gamma_{\text{eff}})_{\max} = \frac{\Delta\gamma}{2}\left(\frac{E}{E_c} + \frac{E_c}{E}\right).$$

The maximum occurs for $h_0 = h_c$:

$$q_0 h_c = g^{-1/2}\left[\left(\frac{E_c}{E}\right)^2 - 1\right]^{1/2}.$$

Thus if, e.g., $E_c/E \approx 10$, the maximal pull-off force should be ~ 5 times larger than for perfectly smooth surfaces. This type of enhancement of $\Delta\gamma_{\text{eff}}$ has been deduced from rolling friction experiments[13] using very soft rubbers (with $E \approx 0.07$ MPa), but the interpretation of the data is complicated by the fact that the rubber is not perfectly elastic, but rather exhibit (rate-dependent) viscoelastic properties.

For most "normal" solids, $\Delta\gamma \approx Ea$, where a is an atomic distance (of order ~ 1 Å) and E the elastic modulus. Thus, $\delta \sim a \sim 1$ Å and typically $1/q_0\delta \sim 10^5$ so that the (repulsive) energy stored in the elastic deformation field in the solids at the interface, and proportional to $f(H)$, largely overcomes the increase in adhesion energy derived from the roughness induced increase in the contact area, described by the term $(q_0 h_0)^2 g(H)/2$.

Let us note the following very important fact. Many solids respond in an elastic manner when exposed to rapid deformations, but flow plastically on long enough time scales. This is clearly the case for non-cross-linked glassy polymers, but it is also to some extent the case for rubbers with cross links. The latter materials behave as relative hard solids when exposed to high-frequency perturbations, while they deform as soft solids when exposed to low-frequency perturbations. Thus, when such a solid is squeezed rapidly against a substrate with roughness on many different length scales, a large amount of elastic energy may initially be stored in the local (asperity induced) deformation field at the interface. However, if the system is left alone (in the compressed state) for some time, the local stress distribution at the interface will decrease (or relax, because of thermal excitation over the barriers), while the area of real contact simultaneously increases. This will result in an increasing adhesion bond
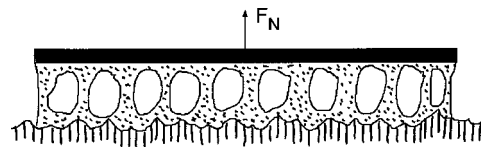
between the solids, and a decrease in the elastic deformation energy stored in the solids: both effects will tend to increase of the pull-off force. (Note: The elastic energy stored at the interface during the compression phase is almost entirely given back during slow pull-off.) Since we use a frequency independent elastic modulus, such time-dependent effects are, of course, not taken into account in the analysis presented previously.

The interfacial free energy is a sum of the adhesive part U_{ad}, which is proportional to the area of real contact, and the elastic energy U_{el} stored in the strain field at the interface. As long as $\Delta U = U_{\text{ad}} + U_{\text{el}} < 0$, a finite pull-off force will be necessary in order to separate the bodies. When the amplitude of the surface roughness increases, ΔU will in general increase and when it reaches zero, the pull-off force vanishes. Suppose now that an elastic slab has been formed between two solids from a liquid "glue layer," which has transformed to the solid state after some hardening time. For example, many glues consist of polymers which originally are liquid, and slowly harden, e.g., via the formation of cross bridges. In this case, if the original liquid wets the solid surfaces, it may penetrate into all surface irregularities and make intimate contact with the solid walls, and only thereafter harden to the solid state. Ideally, this will result in a solid elastic slab in perfect contact with the solid walls, and *without any interfacial elastic energy stored in the system*, i.e., with $U_{\text{el}} = 0$. (In practice, shrinkage stresses may develop in the glue layer, which will lower the strength of the adhesive joint.) Thus the last term in the expression for $\Delta\gamma_{\text{eff}}$ vanishes, and $\Delta\gamma_{\text{eff}}$ will increase with increasing surface roughness in proportion to the surface area. This will result in an increase in the pull-off force, but finally the bond breaking may occur inside the glue film itself,[14] rather than at the interface between the glue film and the solid walls (see Fig. 5); from here on no strengthening of the adhesive bond will result from further roughening of the confining solid walls.

Thus, the fundamental advantage of using liquidlike glues (which harden after some solidification time), compared to pressure-sensitive adhesives which consist of thin solid elastic ($E \approx 10^4 - 10^5$ Pa) films, and which develop tack only when squeezed between the solid surfaces, is that in the former case no elastic deformation energy is stored at the interface (which would be given back during the removal process and hence reduce the strength of the adhesive bond), while this may be the case for the latter type of adhesive, unless the interfacial stress distribution is able to relax toward the stress-free state (which requires the absence of cross links, or such a low concentration of cross links that "thick" liquidlike polymer layers occur at the interfaces).

If we define

FIG. 5. When the interaction between the "glue" film and the substrate is "strong," the separation may involve internal rupture of the glue film rather than detachment at the interface.

$$\alpha = (q_0 h_0)^2 g(H)/2, \tag{15}$$

$$\theta = \frac{E h_0^2 q_0}{4(1-\nu^2)\Delta\gamma}, \tag{16}$$

then Eq. (12) takes the form

$$\Delta\gamma_{\text{eff}} = \Delta\gamma(1 + \alpha - \theta f(H)). \tag{17}$$

In what follows we will assume $\alpha \ll 1$ and neglect the α term in Eq. (17). Note that without a low-distance cutoff (i.e., $q_1/q_0 = \infty$), $f(H) = \infty$ for $H \leq 1/2$ and it is clear that in this limiting case no adhesive interaction will occur *independent* of the magnitude of $\Delta\gamma$. (This statement is only strictly true as long as the attractive interaction responsible for $\Delta\gamma$ is assumed to have zero spatial extent.) The physical reason is that in this case the elastic energy stored in the deformation fields in the solids will always be larger than the adhesion energy which is proportional to $\Delta\gamma$. Note that for the important case $H \approx 1/2$, and if $\alpha \ll 1$, Eq. (17) gives

$$\Delta\gamma_{\text{eff}} \approx \Delta\gamma\left[1 - \frac{1}{2}\theta\ln\left(\frac{q_1}{q_0}\right)\right], \tag{18}$$

which (for $q_1/q_0 \gg 1$) is rather insensitive to the actual magnitude of q_1/q_0.

In the above-mentioned study we have compared the free energies for the case of complete contact between the rubber and the substrate, with the case when no contact occur. In reality, for large enough surface roughness the free energy may be minimal for partial contact. Indeed, the experimental results of Fuller and Tabor[3] suggest this to be the case (see Sec. IV), and in Sec. V we will consider this case in greater detail.

IV. CONTACT MECHANICS WITH ADHESION: COMPLETE CONTACT

We consider the simplest possible case, namely a rectangular elastic block with flat surfaces, in contact with a nominally flat substrate surface. Assume that the block has a height $L_z = L$ and the bottom surface area $A_0 = L_x L_y$. Assume that the upper surface of the block is camped in the perpendicular direction [indicated by the thin (rigid) black slab in Fig. 5], and pulled vertically with the force F_N. We assume that the bond between the block and the substrate breaks via the propagation of an interfacial crack, which may nucleate either (a) at the periphery of the contact area, or (b) at some point inside the contact area (see Fig. 6). In the following we will make the simplifying assumption that the stress in the block far away from the crack is uniaxial, as would be the case if the elastic film would be able to slide in the parallel direction. Thus, if the upper clamped surface is moved upwards with the distance u, then the elastic energy stored in the block (in the absence of the crack) is $A_0 L E(u/L)^2/2$. Thus, assuming zero surface roughness, we write the potential energy for the system as (see Fig. 6)

$$U = -F_N u + \frac{1}{2}A_0 L E\left(\frac{u}{L}\right)^2 - A_0\Delta\gamma.$$
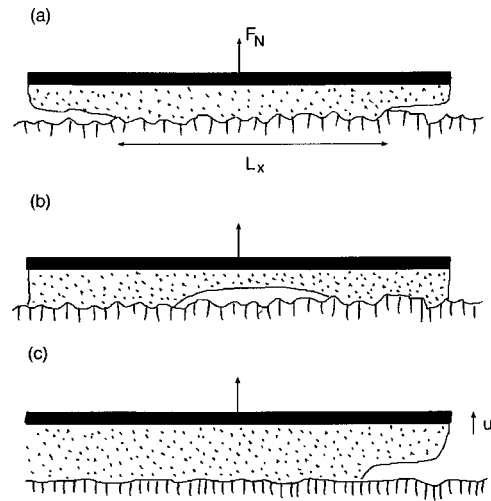
Minimizing this expression with respect to u gives

FIG. 6. The block–substrate bond is broken by a crack propagating (a) from the periphery of the contact area, or (b) by a crack which has nucleated somewhere in the contact area, e.g., at an imperfection. (c) Definition of the displacement u.

$$F_N = A_0 E u/L. \tag{19}$$

Now, consider $F_N > 0$. The block–substrate bond clearly cannot break if the elastic energy stored in the block is smaller than the surface energy $A_0\Delta\gamma$ created when the block–substrate bond is broken. We expect the bond between the block and the substrate to break when the elastic energy becomes equal to the surface energy, i.e.,

$$\frac{1}{2}A_0 L E\left(\frac{u}{L}\right)^2 = A_0\Delta\gamma$$

or

$$u = \left(\frac{2\Delta\gamma L}{E}\right)^{1/2}$$

and the pull-off force $F_N = F_c$ [from Eq. (19)]:

$$F_c = A_0\left(\frac{2\Delta\gamma E}{L}\right)^{1/2}. \tag{20}$$

The above-used condition to determine the adhesion force F_c, namely that the elastic energy stored in the block equals the created surface energy, is only valid if the strain field in the block is constant (which is the case in the present simple geometry, but not in more complex geometries, e.g., when a ball is squeezed against a flat substrate). In general, this condition must be replaced with the condition that U is stationary as the contact area is varied, i.e., $\partial U/\partial A_0 = 0$. We note that the present theory of adhesion is really a Griffith calculation in fracture mechanics.[15]

The free energy minimization calculation performed previously can be extended to more complicated systems. For example, when an elastic sphere (radius R_0) is in contact with a substrate, the pull-off force becomes (see Appendix A)

$$F_c = (3\pi/2)R_0\Delta\gamma. \tag{21}$$

This result was first derived by Sperling[16] and (independently) by Johnson, Kendall, and Roberts.[4] Kendall has reported similar results for other geometries of interest.[17]
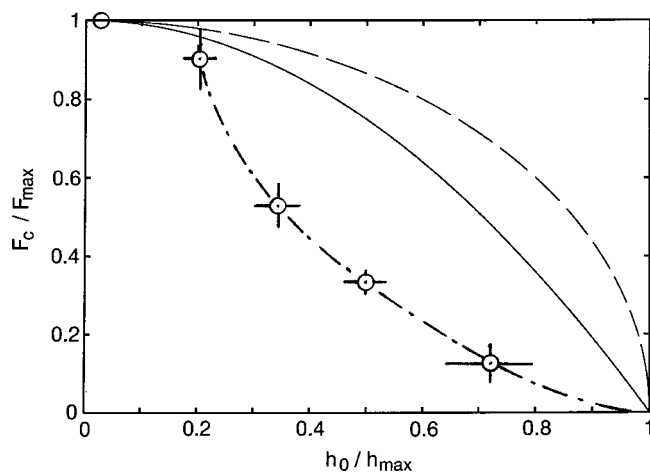
FIG. 7. The pull-off force, F_c, in units of the maximum pull-off force, as a function of the surface roughness amplitude h_0. The solid and dashed lines are theoretical curves for a spherical ball and for a rectangular block, respectively, assuming complete contact in the nominal contact area (see the text). The circles are experimental data from Ref. 3, and the dotted-dashed line is a guide to the eye.

Consider now the same problems as previously, but assume that the substrate surface has roughness described by the function $z = h(\mathbf{x})$. We now study how the adhesion force is reduced from the ideal value (20) or (21) as the amplitude of the surface roughness is increased. Let us first assume that the adhesive interaction is so strong that the elastic solid is in contact with the substrate everywhere. In this case we can still use result (20), but with $\Delta\gamma$ replaced by $\Delta\gamma_{\text{eff}}$ as given by Eq. (13). Thus if $\alpha \ll 1$ we get for a rectangular block in contact with a nominally flat substrate:

$$F_c = (F_c)_{\text{max}}[1 - \theta f(H)]^{1/2}, \tag{22}$$

where $(F_c)_{\text{max}}$ is given by Eq. (20). Similarly, for an elastic sphere in contact with a nominally flat substrate

$$F_c = (F_c)_{\text{max}}[1 - \theta f(H)], \tag{23}$$

where $(F_c)_{\text{max}}$ is given by Eq. (21). Note that $F_c \to 0$ as $\theta f(H) \to 1$; when $\theta f(H) = 1$ the elastic energy stored in the deformation field at the interface equals the surface energy $\Delta\gamma A$ (where A is the area of real contact), and no "external" energy is necessary in order to break the block–substrate bond. When $\theta f(H) > 1$, the elastic energy stored at the interface is larger than the gain in surface energy which would result from the direct contact between the block and the substrate; this state is stable only if the solids are squeezed against each other with an external force.

In Fig. 7 we compare the present theory with the experimental results of Fuller and Tabor for several glass surfaces with different surface roughness rms amplitude. (We assume here, and in what follows, that the roughness parameters H
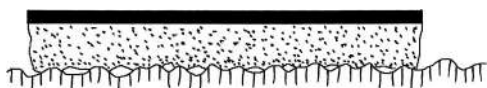

FIG. 8. For "large" surface roughness the free energy is minimal (when $F_N = 0$) for *partial* rubber–substrate contact, rather than for complete contact.
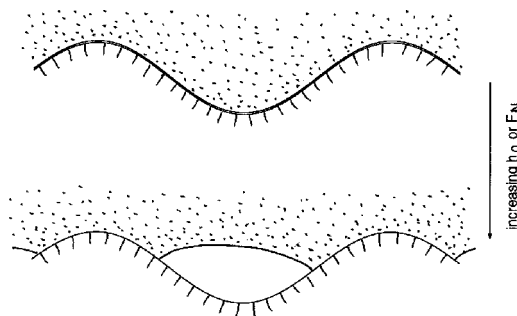

FIG. 9. The detachment transition (schematic). For small surface roughness, complete contact occurs in the nominal contact area (top), while for large surface roughness there is a jump to partial contact (bottom).

and q_0 are the same for all the different surfaces.) The solid and dashed lines are theoretical curves for a spherical ball and for a rectangular block, respectively, assuming complete contact in the nominal contact area. The agreement between theory and experiment is good for small rms roughness values, $h_0/h_{\text{max}} < 0.2$ (where h_{max} is the h_0 value for which $\theta f(H) = 1$, i.e., $h_{\text{max}} = 2[(1 - \nu^2)\Delta\gamma/Eq_0 f(H)]^{1/2}$), but for large h_0 the experimental pull-off force falls somewhat below the theoretical prediction. This may be due to the fact that for "large" surface roughness the free energy is minimal (when $F_N = 0$) for *partial* rubber–substrate contact, rather than for complete contact (or zero contact), as assumed previously, see Fig. 8.

In fact, for surface roughness on a single length scale, e.g., $z = h_0 \cos(q_0 x)$, it is easy to convince oneself that there will be a discontinuous *detachment transition* from complete contact to partial contact (Fig. 9) when the pull-off force (or the amplitude of the roughness h_0) is increased. This can be seen directly if we consider a very narrow detached region at the bottom of a valley as in Fig. 10. We can treat the detached region as a crack of width b. As is well known in that case[15] the stress at the crack edges will be proportional to $(b/r)^{1/2}$, where r is the distance away from a crack edge. Thus, the local stress at a crack tip will increase with the width b of the crack, so that after nucleation the crack will expand to a finite size. Thus partial detachment on a single length scale is a first-order transition. We have performed a preliminary study[18] [for a $\cos(q_0 x)$ profile] which shows that on increasing the pull-off force (or increasing h_0 at vanishing external force) the system first "flips" from a state with com-
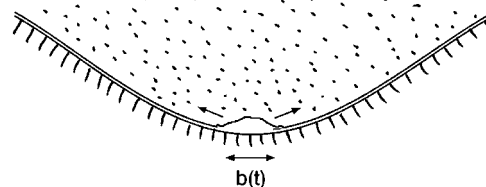

FIG. 10. When the amplitude h_0 of the surface roughness, or the pull-off force F_N, is increased beyond a critical value, a discontinuous detachment transition takes place from a state of complete contact to partial contact. The transition can be considered as resulting from the nucleation of a crack at the bottom of the valley, followed by rapid expansion of the crack until it reaches a width of order $\sim \lambda/2$.

plete contact to another "asperity contact" state (Fig. 8) where the width of the contact region is less than $\lambda/2$ as indicated in Fig. 9 (bottom).

Real surfaces do, of course, exhibit roughness on many different length scales, and the relation between the pull-off force and the center of mass displacement is therefore likely to be continuous for most systems of practical interest. Nevertheless, during pull-off rapid flip events may take part at the interface, where the solids first undergo local detachment in the valleys of the roughness profile, followed at large enough pull-off force by complete detachment, the asperity contact areas detaching the last. Because of the long-range nature of the elastic interaction, one may expect a cooperative behavior of the detachment process, where detachment in one local area may induce detachment in other interfacial surface areas. Fuller and Roberts[13] have studied the line of peeling (crack edge) during pull off (see also Ref. 19). For smooth surfaces the line is straight and peeling occurs uniformly. Roughening the counterface makes the line increasingly irregular, and peeling is intermittent, involving short sections of the front at a time. This mode of behavior indicates variation in the strength of the adhesion over the contact area as a result of the irregularly fluctuating surface roughness. The exact nature of the detachment process and its possible collective behavior represents an interesting problem for future studies.

Fuller and Tabor performed experiments with three different rubbers with very different elastic modulus E. The dependence of the adhesion on the magnitude of E is in good agreement with the above-presented theoretical predictions.

V. CONTACT MECHANICS WITH ADHESION: PARTIAL CONTACT

We will now show that the discrepancy between theory and experiment for $h_0/h_{max}>0.2$ in Fig. 7 is due to rubber–substrate detachment, which reduces the area of real contact and the pull-off force for large surface roughness. We assume again that the rough surface is a self-affine fractal with a long distance cut-off $\lambda_0=2\pi/q_0$. We will refer to the "asperities" on the length scale λ_0 as the macroasperities. The macroasperities are covered by shorter wavelength roughness down to the lower cutoff length $\lambda_1=2\pi/q_1$. We assume the contact between the rubber and the substrate to involve just a fraction of the macroasperities. We will refer to a contact region between a macroasperity and the substrate as the "asperity contact area." We now make the basic assumption that the rubber is in direct contact with the substrate in the asperity contact areas and we will take into account the short-wavelength surface roughness simply by using the effective $\Delta\gamma_{eff}$ introduced previously, where, however, the surface roughness on the length scale $\sim\lambda_0$, which now is treated explicitly, has been removed from the surface roughness profile when calculating $\Delta\gamma_{eff}$.[20] Thus, the present problem reduces to the study of Fuller and Tabor, except that we must replace $\Delta\gamma$ with $\Delta\gamma_{eff}$. Since $\Delta\gamma_{eff}\to0$ as $\theta f(H)\to1$ it is still true that the pull-off force vanishes when $\theta f(H)=1$. However the pull-off force before detachment will not be the same.
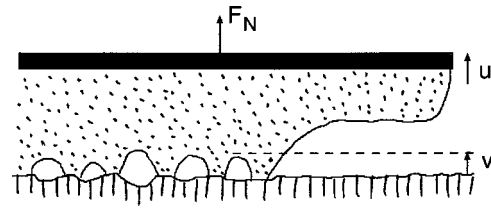

FIG. 11. Definition of the displacements u and v.

Let us consider the case of a rectangular block in contact with a rough substrate. The potential energy for the system is:

$$U=-F_N u+\frac{1}{2}A_0 LE\left(\frac{u-v}{L}\right)^2+V(v),\tag{24}$$

where u and v are the (lateral averaged) displacements of the upper and lower surface of the block (see Fig. 11), and the block–substrate asperity interaction energy is

$$V=n_0 A_0\int_{z_c}^{\infty}dz\;\phi(z)U_{asp}(z-v).\tag{25}$$

n_0 is the concentration of macroasperities, U_{asp} the interaction energy between a substrate asperity and the elastic block, and z_c is the smallest asperity height for which block–substrate contact occurs. The asperity height distribution $\phi(z)$ is assumed to be Gaussian so that[21]

$$\phi(z)=(\pi h_0^2)^{-1/2}e^{-(z/h_0)^2}.\tag{26}$$

The radius r of an asperity contact region can be related to the compression $h=z-v$ via (during pull-off, $h<0$) (see Appendix A and Ref. 4)

$$\bar{h}=\bar{r}^2-(2\bar{r})^{1/2}.\tag{27}$$

Here $r=\alpha R\bar{r}$ and $h=\alpha^2 R\bar{h}$, where $\alpha=(\pi\Delta\gamma_{eff}/E^*R)^{1/3}$ (where $\Delta\gamma_{eff}=\Delta\gamma[1-\theta f(H)]$), defines the dimensionless quantities $\bar{r}$ and $\bar{h}$. The energy [see Eq. (A11)]

$$U_{asp}=E^*R^3\alpha^5(\tfrac{8}{15}\bar{r}^5+\bar{r}^2-\tfrac{4}{3}\bar{r}^3(2\bar{r})^{1/2}).\tag{28}$$

Substituting Eqs. (26) and (28) in Eq. (25) and defining $z=\alpha^2 R\bar{z}$ gives

$$V=n_0 A_0\int_{\bar{z}_c}^{\infty}d\bar{z}\,\alpha^2 R(\pi h_0^2)^{-1/2}e^{-\bar{z}^2(\alpha^2 R/h_0)^2}$$

$$\times E^*R^3\alpha^5\left(\frac{8}{15}\bar{r}^5+\bar{r}^2-\frac{4}{3}\bar{r}^3(2\bar{r})^{1/2}\right).\tag{29}$$

Now, let us change integration variable, from $\bar{z}$ to $\bar{r}$. Using $\bar{z}=\bar{h}+v/\alpha^2 R$ and Eq. (27) gives

$$d\bar{z}=d\bar{r}[2\bar{r}-(2\bar{r})^{-1/2}].$$

Thus,

$$V = n_0 A_0 \int_{\bar{r}_c}^{\infty} d\bar{r} [2\bar{r} - (2\bar{r})^{-1/2}] \alpha^2 R (\pi h_0^2)^{-1/2}$$

$$\times e^{-[\bar{r}^2 - (2\bar{r})^{1/2} + v/\alpha^2 R]^2 (\alpha^2 R/h_0)^2}$$

$$\times E^* R^3 \alpha^5 (\tfrac{8}{15} \bar{r}^5 + \bar{r}^2 - \tfrac{4}{3} \bar{r}^3 (2\bar{r})^{1/2}). \tag{30}$$

We must now determine $\bar{r}_c$. Under conditions of increasing negative load, separation of the surfaces occur when $dF/dh = 0$ which implies $\bar{r}_c = (9/8)^{1/3}$. However, under condition of increasing displacement, stable equilibrium prevails until $dF/dh = \infty$, which implies $\bar{r}_c = 1/2$ (see Appendix A). This latter condition is relevant in the present case. Note that

$$\Theta = \frac{\alpha^2 R}{h_0} = \left(\frac{\pi \Delta \gamma_{\text{eff}} R^{1/2}}{E^* h_0^{3/2}} \right)^{2/3}$$

$$\approx \left(\frac{\pi}{4} \right)^{2/3} \theta^{-2/3} [1 - \theta f(H)]^{2/3}, \tag{31}$$

where we have assumed that $1/R \approx q_0^2 h_0$. If we denote $\bar{r} = x$ for simplicity, then Eq. (30) gives

$$V = -n_0 A_0 \Delta \gamma_{\text{eff}} R h_0 \bar{V}(\theta, v/h_0), \tag{32a}$$

$$\bar{V} = \sqrt{\pi} \Theta^2 \int_{1/2}^{\infty} dx [2x - (2x)^{-1/2}] e^{-[\Theta(x^2 - (2x)^{1/2}) + v/h_0]^2}$$

$$\times (\tfrac{8}{15} x^5 + x^2 - \tfrac{4}{3} x^3 (2x)^{1/2}). \tag{32b}$$

Minimizing Eq. (24) with respect to u gives

$$F_N = A_0 E(u - v)/L. \tag{33}$$

Similarly, minimization with respect to v gives

$$A_0 E \frac{v - u}{L} + \frac{dV}{dv} = 0.$$

Using Eq. (33) this gives

$$F_N = \frac{dV}{dv}. \tag{34}$$

Note that F_N only depends on θ and v/h_0. In Fig. 11 we show $\bar{F}_N = h_0 d\bar{V}(\theta, v/h_0)/dv$ as a function of v/h_0 for $\theta = 0.3$ and 0.6 [and with $f(H) = 1$]. Fuller and Tabor[3] determined the pull-off force from curves such as in Fig. 12 by the condition $dF_N/dv = 0$. However, this is usually not the correct condition: If the elastic energy in the block becomes equal to the interfacial energy $A_0 \Delta \gamma_{\text{eff}}$ before the condition $dF_N/dv = 0$ is satisfied, then the pull-off force will be determined by $U_{\text{el}} = -U_{\text{ad}}$. The latter condition is relevant if the size of the block is large enough (see the following), which will be assumed to be the case in what follows.

The pull-off force is determined by the condition that the elastic energy stored in the system is just large enough to break the attractive block–substrate bond. This gives

$$\frac{1}{2} A_0 L E \left(\frac{u - v}{L} \right)^2 + V(v) = 0,$$
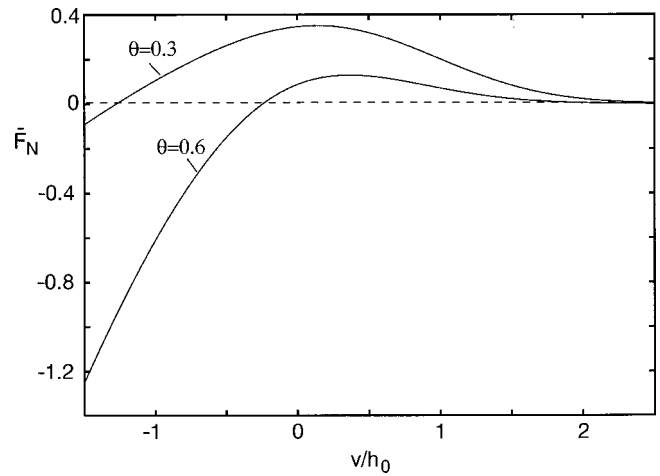
or, using Eq. (33),

FIG. 12. The normalized force $\bar{F}_N = h_0 d\bar{V}(\theta, v/h_0)/dv$ as a function of the displacement v (in units of h_0) of the bottom surface of the block. For $\theta = 0.3$ and 0.6, and with $f(H) = 1$.

$$\frac{1}{2} A_0 L E \left(\frac{F_c}{A_0 E} \right)^2 + V(v) = 0. \tag{35}$$

Using Eqs. (32a), (35), and $(Rh_0 n_0)^{1/2} \approx (n_0/q_0^2)^{1/2} \approx 1/2\pi$ gives

$$F_c \approx A_0 \left(\frac{2\Delta \gamma_{\text{eff}} E}{L} \right)^{1/2} \frac{1}{2\pi} [\bar{V}(\theta, v/h_0)]^{1/2},$$

or, comparing to Eq. (20),

$$F_c \approx (F_c)_{\text{max}} [1 - \theta f(H)]^{1/2} [\bar{V}(\theta, v/h_0)]^{1/2}/2\pi. \tag{36}$$

Using Eqs. (34) (with $F_N = F_c$) and (36) gives an equation for v/h_0. Now, since $F_c \sim L^{-1/2}$, in the limit of large L, F_c will be very small and we can obtain the relevant v/h_0 to be used in $\bar{V}(\theta, v/h_0)$ in Eq. (36) by putting $F_N = 0$ in Eq. (34), i.e., $dV/dv = 0$. In Fig. 13 (dashed line) we show the result-
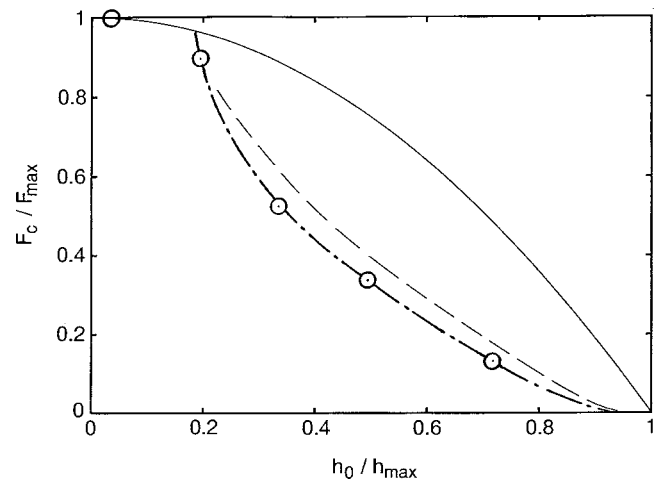

FIG. 13. Solid line: The relation between the pull-off force and the roughness amplitude, assuming complete contact between the ball and the substrate in the nominal contact area. Dashed line: The relation between F_c and h_0 for partial contact for $f(H) = 1.0$. Points are the same experimental data as Fig. 7.
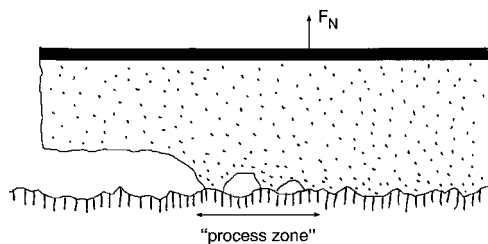
FIG. 14. The transition from complete contact to detached area may involve a region of partial detachment, called the "process zone."

ing pull-off force as a function of h_0. Note that there are no fitting parameters in the theory, and that the calculation is in good agreement with the experimental trend, especially near h_{max}. In fact, the present model calculation is only valid when the asperity contact area is very small compared to λ^2 (only then is the JKR theory valid), i.e., the theory holds strictly only for h_0 close to (but below) h_{max}. Thus, it is not surprising that the experimental reduction in the pull-off force for h_0 well below h_{max} is somewhat larger than predicted by the theory. Nonetheless, the overall qualitative form of detachment-induced pull-off force reduction is in good agreement with the experimental data.

Let us close this section by discussing the two alternative pull-off conditions (a) $dF_N/dv = 0$ and (b) $U_{el} = -U_{ad}$ (or, more generally, $\partial U_{tot}/\partial A_0 = 0$). Condition (a) corresponds to a uniform (over the nominal contact area) detachment of the block–substrate asperity contact areas, while (b) corresponds to crack propagation, either from the periphery of the nominal contact area, or from some point (crack nucleation center) inside the contact area. As stated earlier, if the block is big enough, case (b) will correspond to the smallest pull-off force, and will hence prevail.

VI. DISCUSSION

Consider an elastic block on a substrate. When the thickness $L = L_z$ of the block increases (but we assume $L_x \gg L_z$ and $L_y \gg L_z$), the pull-off stress F_c/A_0 decreases as $\sim L^{-1/2}$, see Eq. (20). Thus, for large L the (average) perpendicular stress at the block–substrate interface will be very small (this is the reason why glue films should be very thin in order to give a maximal pull-off force[22]), and the magnitude of the surface roughness alone will determine whether the elastic media is in complete contact with the substrate or only in partial contact. (The same is true if instead of a block, an elastic ball is in contact with the substrate. In this case the average stress in the contact area at pull-off decreases as $R_0^{-1/3}$, with increasing radius R_0 of the ball.) Of course, stress concentration will occur at the crack tip, so that partial detachment may occur in a small region around the crack tip, even if complete contact occurs far away from the tip inside the contact region, see Fig. 14. In the latter case, even if the crack propagates slowly, at the crack tip rapid flip events may occur as the individual block–substrate asperity contact areas are broken. This may lead to large energy dissipation, as the elastic energy stored in the elongated bridges is lost during the rapid flip events, and under those circumstances the pull-off force will be much larger than predicted by Eq.

(20) [or Eq. (22)]. These rapid flips clearly did not play any major role in the experiments of Fuller and Tabor, but do occur in many practical applications involving glues. Usually the standard theory of crack motion can be used to treat these more complicated cases, but $\Delta\gamma$ must now be replaced by the strain energy release rate G, which is the energy needed to propagate the crack by one unit area. When only reversible processes occur at the crack tip (no rapid flip processes), $G = \Delta\gamma$ (or $\Delta\gamma_{eff}$ for rough surfaces) but if cavity formation and fibrillar structures occur, G may be 1000 times (or more) larger than $\Delta\gamma$. The topic of designing glues exhibiting large G is of great practical importance.

The region in space where the block–substrate detachment occurs at a crack edge is usually called the crack "process zone" (see Fig. 14). In some extreme cases the width of this zone may become comparable to (or larger than) the width L_x (or L_y) of the nominal contact region. In this case it is no longer correct (or useful) to think about the block–substrate bond breaking as involving crack propagation. This seems to be the case for many practical glues. The theoretical treatment of these cases cannot be based on the theory of crack motion, but involves new physics, such as the microscopic site of cavitation (i.e., the question whether the nucleation occurs right at the interface or in the bulk of the glue film), the concentration and spatial distribution of cavities, and the evolution from cavities to fibrilar structures. These processes have been intensively studied recently for a flat probe geometry,[23] where a block with a nominal flat surface is squeezed against a flat substrate covered by a thin (usually $L \approx 100\,\mu m$) polymer film acting as a pressure-sensitive adhesive. After a short contact time the block is removed with a constant pull-off velocity, and the relation between the strain and stress is studied as function of time, while snapshot pictures show the geometrical evolution of the adhesive film. It is found that very soft adhesive undergoes cavitation and fibrillation processes when subjected to a tensile stress. A slight degree of cross linking is beneficial for the stability of the fibrils, but excessive cross linking can lead to a premature failure of the fibrils, therefore significantly reducing the adhesion energy.

The voids first nucleate in the region which was last brought in contact with the probe and thereafter relatively homogeneously over the whole contact area. Nucleation will take place near the maxima in the pull-off force. The cavities usually nucleate at the probe/film interface. The fact that nucleation occurs fairly homogeneously has been interpreted to imply that the negative hydrostatic pressure is fairly homogeneous under the probe surface. We do believe this is indeed correct, but only after the nucleation of the cavities has started (see the following).

Experiments with probe surfaces exhibiting different surface roughness have shown that even when cavitation and stringing occur, the pull-off force increased significantly when going from rough probe surfaces to smooth ones.[23] This is in accordance with the theory presented earlier. Simultaneously, there appeared a striking difference in the morphology of the de-bonding area. Thus, only the rough probe (1.2 μm rms roughness) gave a significant fibrilar structure. The other probe surfaces ($<0.1\,\mu m$ rms rough-
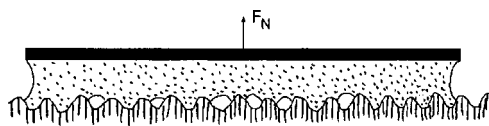
FIG. 15. The external force F_N induce detached areas. The concentration of detached areas is highest in the center of the contact region, where the tensile stress would be highest in the absence of the detached areas. (Schematic.)

FIG. 16. Elastic deformation of the substrate walls during pull-off. (Schematic.)

ness) did not evolve into a fibrilar structure so that, in the end, the adhesion energies (the energy to separate the probe from the substrate) were all quite comparable.

Let us discuss the process of cavity formation. Let us consider a thin polymer film (thickness L) between two flat rigid surfaces. If the polymer is considered as fully incompressible, then the pressure p in the film is approximately[14,23]

$$p = p_{ext} - E\epsilon\left(\frac{r_0^2 - r^2}{L^2}\right), \tag{37}$$

where p_{ext} is the external pressure, $\epsilon = \Delta L/L$ is the strain and r_0 is the radius of the circular contact region. The average pressure $\bar{p} = p_{ext} - E\epsilon r_0^2/2L^2$. It is interesting to note that this pressure distribution is similar to that for an incompressible fluid (e.g., a polymer melt without cross links) (see, e.g., Ref. 1):

$$p = p_{ext} - 3\mu\dot{\epsilon}\left(\frac{r_0^2 - r^2}{L^2}\right), \tag{38}$$

where μ is the viscosity and $\dot{\epsilon} = \dot{L}/L$. In fact, for a periodic oscillating strain, $\dot{\epsilon} = -i\omega\epsilon$, and defining the complex elastic modulus $E(\omega) = -i\omega\mu$, Eq. (38) takes the same form as Eq. (37) except for a factor of 3. For a "nearly" incompressible material, say with the Poisson ratio $\nu = 0.49$, the pressure distribution becomes much flatter.[23] However, the bulk modulus of polymers is of order 10^{10} Pa, while the elastic modulus $E \approx 10^4$ Pa (typical for pressure-sensitive adhesives at low deformation rate) so that $0.5 - \nu \approx 10^{-6}$; under these conditions the pressure distribution in the polymer film will deviate negligibly from that calculated under the assumption of an perfectly incompressible material. We must therefore ask why the macroscopic cavities occur uniformly in the contact area, in spite of the very nonuniform pressure distribution [Eq. (37)] which occurs before the nucleation. We believe that the explanation of this puzzle may be related to detachment, as follows.

First, note that the typical maximal (average) pressure in a pull-off experiment[23] is of order 0.4 MPa. Using Eq. (37) with $L = 100 \mu$m, $r_0 = 1$ cm (so that $r_0/L \approx 100$), and $E = 10^4 - 10^5$ Pa gives the true strain $\epsilon \approx 10^{-3}$ corresponding to the displacement $\Delta L = \epsilon L \approx 0.1 \mu$m. Now, the rms surface roughness of the probe surface was approximately 1 μm. Thus, it is clear that if a low concentration of microscopic *local detachments occurs at the interface when the stress is increased* (see Fig. 9), then this will locally reduce the stress in the contact region. If we assume some characteristic stress ("yield stress") in order to induce a local detachment, the detached areas will be distributed in such a way (see Fig. 15) that a nearly uniform stress may arise in the contact region
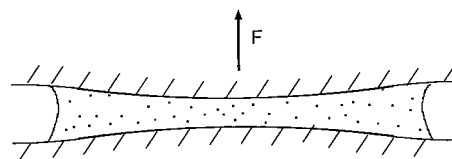
even before any macroscopic detached regions (cavities) can be observed. As the strain is increased further, some of the microscopic detached areas will grow into macroscopic cavities. Hence, when the strain becomes so large (say 0.3) that (macroscopic) cavities can be observed it is clear that they must be more or less uniformly distributed in the contact area. This picture is consistent with the experimental observation that the cavitation stress is directly related to their shear modulus rather than their bulk modulus.[24]

Another mechanism which will also contribute toward making the stress in the contact area uniform has recently been suggested by Creton:[22] The negative pressure at the interface will deform the solid walls in such a way (see Fig. 16) as to make the tensile stress more uniform in the contact area. It is easy to show that this effect is important also for elastically stiff materials such as steel. Thus if a constant pressure acts within a circular region $r < r_0$ on a semi-infinite elastic media, it will result in a displacement u of the center of the circular region given by (see Sec. II) $u \approx (p/E)r_0$. Using the typical values $r_0 = 1$ cm and $p = 1$ MPa, and assuming steel walls so that $E \approx 10^{11}$ Pa gives $u \approx 0.1 \mu$m, which is just of the right order of magnitude in order to give a strong reduction in the pressure at the center of the contact region (see the previous discussion). Thus the substrate bending must be taken into account in any accurate discussion of the pressure distribution in the polymer film during pull-off. We note that this effect is very similar to the deformations occurring during separation of two bodies squeezed together in a liquid, where cavity formation (in the liquid),[25] and elastic deformation of the solid walls have been observed, and also studied theoretically using elastohydrodynamics.

Finally, let us comment on the influence of (small) contamination particles (e.g., dust) on adhesion. It is generally believed that dusty rubber surfaces provide bad adhesion. Now, while this is true in most practical situations, one can imagine cases where it is not true. First, note that the adhesion between two smooth, clean (identical) rubber surfaces is in general very good (see Fig. 17). Now, if a monolayer (or less) of small particles is deposited between the rubber surfaces, this may lead to an even larger pull-off force than for the clean rubber surfaces. This follows from the fact that the particle–rubber adhesion may be stronger than the rubber–rubber adhesion [the van der Waals force is proportional to the polarizability, which is usually larger for hard (heavy) solids (e.g., rock) than for rubbers]. However, if a bilayer (or more) of particles occurs between two rubber surfaces, negligible adhesion is observed, as the separation now occurs at the particle–particle interface. Similarly, a monolayer of par-

(a)

good adhesion

(b)

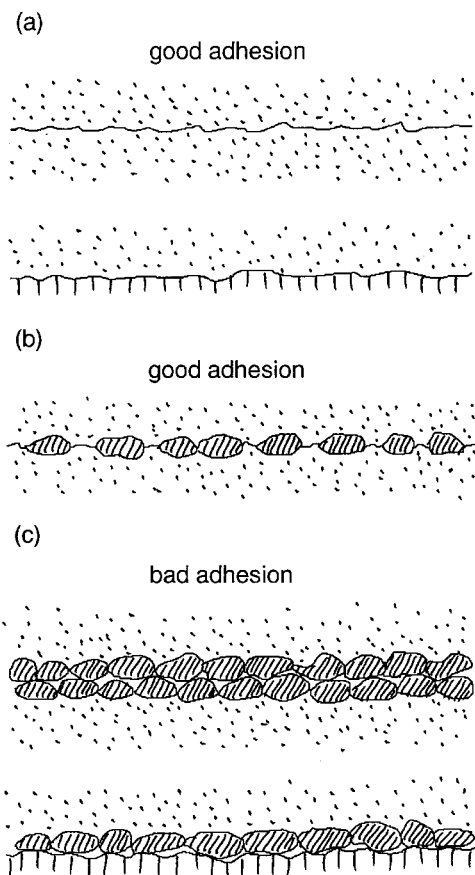good adhesion

(c)

bad adhesion

FIG. 17. The influence of small particles (e.g., dust) on adhesion. (a) The adhesion between two smooth, clean (identical) rubber surfaces, or a rubber surface and a smooth hard substrate, is in general very good. (b) A monolayer (or less) of small particles between two rubber surfaces may lead to a pull-off force which is even larger than for the clean rubber surfaces (see the text). (c) A bilayer (or more) of particles between two rubber surfaces results in negligible adhesion. Similarly, a monolayer of particles at the interface between a hard solid and rubber results in negligible adhesion.

ticles at the interface between a hard solid and rubber will result in negligible adhesion.

VII. SUMMARY AND CONCLUSION

We have studied the influence of surface roughness on the adhesion of elastic solids. Most real surfaces have roughness on many different length scales, and this fact has been taken into account in our study. We have considered in detail the case when the surface roughness can be described by a self-affine fractal, and shown that when the fractal dimension $D_f > 2.5$, the adhesion force may be strongly reduced. We studied the behavior of the block–substrate pull-off force as a function of roughness. For single scale roughness we find a partial detachment transition before full detachment. Finally we studied the full detachment transition for the self-affine fractal surface, and found that total detachment is characterized by exactly the same parameter θ as in the simpler theory of Fuller and Tabor. The partial detachment which occurs before full detachment, however, results in a very substantial reduction in the pull-off force prior to full detachment. That is in good qualitative agreement with experimental data.
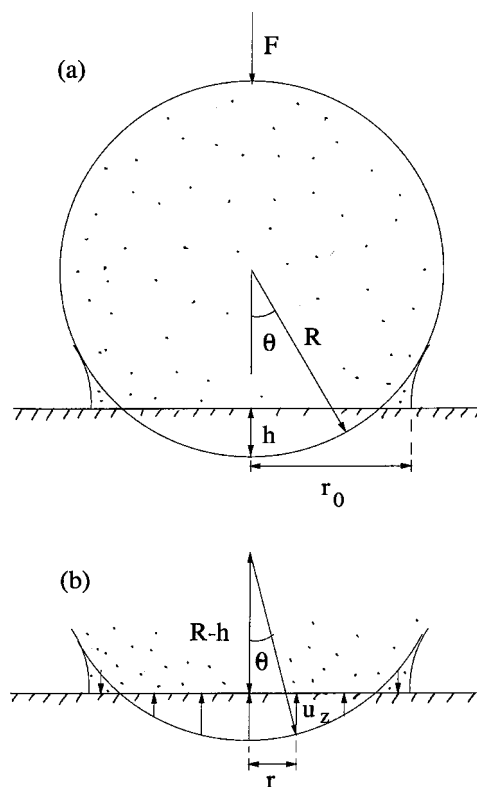
(a)

(b)

FIG. 18. A rubber ball squeezed against a flat rigid substrate.

ACKNOWLEDGMENTS

APPENDIX A

In this appendix we present, for the reader's convenience, a short derivation of the JKR theory. Consider an elastic sphere (radius R) in contact with a rigid flat solid surface (see Fig. 18).

We assume that there is an attractive interaction between the two solids so that the sphere deforms elastically at the interface forming a "neck" as indicated in the Fig. 18. Let r_0 be the radius of the (circular) contact area and assume that $h \ll R$, where $R - h$ is the separation between the center of the sphere and the substrate (see Fig. 18). In order for the deformed elastic sphere to take the shape indicated in Fig. 18, the surface of the sphere must displace as indicated by the arrows in Fig. 18 and given by the relation

$$u_z = h - R(1 - \cos \theta).$$

But since $R \sin \theta = r$ we get

$$\cos \theta = [1 - (r/R)^2]^{1/2} \approx 1 - r^2/2R^2$$

and thus

$$u_z \approx h \left(1 - \frac{r^2}{2hR} \right), \tag{A1}$$

which is valid for $0 < r < r_0$. Let us now determine the pressure distribution which gives rise to the displacement (A1). Since $h \ll R$ (and $r_0 \ll R$) we can determine the pressure distribution under the assumption that the surface of the sphere is locally flat. Using the theory of elasticity, it has been shown that when the surface of a semi-infinite elastic solid is exposed to the pressure

$$\sigma = \sigma_0 \left(1 - \frac{r^2}{r_0^2} \right)^{-1/2} + \sigma_1 \left(1 - \frac{r^2}{r_0^2} \right)^{1/2} \tag{A2}$$

for $r < r_0$, and zero otherwise, then the elastic deformation field (for $r < r_0$) becomes (see, e.g., Ref. 26)

$$u_z = \frac{\pi r_0}{E^*} \left[\sigma_0 + \frac{1}{2} \sigma_1 \left(1 - \frac{r^2}{2r_0^2} \right) \right], \tag{A3}$$

where $E^* = E/(1 - \nu^2)$. Comparing Eq. (A3) with Eq. (A1) gives

$$\sigma_0 = \frac{E^*}{\pi} \left(\frac{h}{r_0} - \frac{r_0}{R} \right), \tag{A4}$$

$$\sigma_1 = \frac{E^*}{\pi} \frac{2r_0}{R}. \tag{A5}$$

Let us calculate the elastic energy stored in the deformation field in the elastic sphere in the vicinity of the substrate. This can be obtained using the general formula

$$U_{el} = \frac{1}{2} \int d^2x \, \sigma(\mathbf{x}) u_z(\mathbf{x}), \tag{A6}$$

where the integral is over the surface area $r < r_0$. Substituting Eqs. (A2) and (A3) in Eq. (A6) gives

$$U_{el} = \pi h \int_0^{r_0} dr \, r \left[\sigma_0 \left(1 - \frac{r^2}{r_0^2} \right)^{-1/2} + \sigma_1 \left(1 - \frac{r^2}{r_0^2} \right)^{1/2} \right]$$
$$\times \left(1 - \frac{r^2}{2hR} \right).$$

If we introduce $\xi = 1 - r^2/r_0^2$ we get

$$U_{el} = \frac{\pi h r_0^2}{2} \int_0^1 d\xi (\sigma_0 \xi^{-1/2} + \sigma_1 \xi^{1/2}) \left[1 - \frac{r_0^2}{2hR}(1 - \xi) \right]$$
$$= \frac{\pi h r_0^2}{2} \left[\left(2 - \frac{r_0^2}{hR} \right) \left(\sigma_0 + \frac{\sigma_1}{3} \right) + \frac{r_0^2}{hR} \left(\frac{\sigma_0}{3} + \frac{\sigma_1}{5} \right) \right]. \tag{A7}$$

Substituting Eqs. (A4) and (A5) in Eq. (A7) gives after some simplifications

$$U_{el} = E^* \left(h^2 r_0 - \frac{2}{3} \frac{h r_0^3}{R} + \frac{1}{5} \frac{r_0^5}{R^2} \right).$$

In order to determine the radius r_0 of the contact area, we must minimize the total energy under the constraint that the

$h = \text{const}$. The total energy is given by the elastic energy plus the change in the surface energy, $-\Delta \gamma \pi r_0^2$, so that

$$U_{tot} = E^* \left(h^2 r_0 - \frac{2}{3} \frac{h r_0^3}{R} + \frac{1}{5} \frac{r_0^5}{R^2} \right) - \Delta \gamma \pi r_0^2.$$

Let us introduce dimensionless variables. If we define $\alpha = (\pi \Delta \gamma / E^* R)^{1/3}$ and introduce $r_0 = \alpha R \bar{r}_0$ and $h = \alpha^2 R \bar{h}$ then the total energy takes the form

$$U_{tot} = E^* R^3 \alpha^5 (\bar{h}^2 \bar{r}_0 - \tfrac{2}{3} \bar{h} \bar{r}_0^3 + \tfrac{1}{5} \bar{r}_0^5 - \bar{r}_0^2). \tag{A8}$$

The force F is given by

$$F = -\frac{\partial U_{tot}}{\partial h} = -\frac{1}{\alpha^2 R} \frac{\partial U_{tot}}{\partial \bar{h}}$$
$$= E^* R^2 \alpha^3 \left(2 \bar{h} \bar{r}_0 - \frac{2}{3} \bar{r}_0^3 \right). \tag{A9}$$

The condition $\partial U_{tot}/\partial \bar{r}_0 = 0$ takes the form

$$(\bar{h} - \bar{r}_0^2)^2 = 2 \bar{r}_0$$

with the solutions

$$\bar{h} = \bar{r}_0^2 \pm (2 \bar{r}_0)^{1/2}. \tag{A10}$$

The two $\pm$ solutions correspond to different total energies, and the correct solution is the one which minimizes the total energy. Substituting Eq. (A10) in Eq. (A8) gives

$$U_{tot} = E^* R^3 \alpha^5 (\tfrac{8}{15} \bar{r}_0^5 + \bar{r}_0^2 \pm \tfrac{4}{3} \bar{r}_0^3 (2 \bar{r}_0)^{1/2}). \tag{A11}$$

Thus the minus sign solution gives the lowest energy.

Under conditions of increasing negative load, separation of the surfaces occurs when $dF/dh = 0$ or, equivalently, $dF/dr_0 = 0$. Using Eqs. (A9) and (A10) this gives $\bar{r}_0 = \bar{r}_c = (9/8)^{1/3}$ and the pull-off force $F = -(3\pi/2)R\Delta \gamma$. However, under condition of increasing displacement, stable equilibrium prevails until $dF/dh = \infty$, which implies $dh/dr = 0$ and from Eq. (A10), $\bar{r}_c = 1/2$.

APPENDIX B

In this appendix we present a more accurate treatment of the averaging of the surface energy term. First note that

$$\langle [1 + (\nabla h)^2]^{1/2} \rangle = \int d^2w \langle \delta(\mathbf{w} - \nabla h) \rangle (1 + w^2)^{1/2}$$
$$= \frac{1}{(2\pi)^2} \int d^2w \int d^2k \langle e^{i\mathbf{k} \cdot (\mathbf{w} - \nabla h)} \rangle \times (1 + w^2)^{1/2}$$
$$= \frac{1}{(2\pi)^2} \int d^2w \int d^2k \, e^{i\mathbf{k} \cdot \mathbf{w}} \langle e^{-i\mathbf{k} \cdot \nabla h} \rangle \times (1 + w^2)^{1/2}.$$

If we assume, as is usually done, that $h(\mathbf{x})$ is a Gaussian random variable, then

$$\langle e^{-i\mathbf{k}\cdot\nabla h}\rangle = \left\langle \exp\left[-i\mathbf{k}\cdot\int d^2 q h(\mathbf{q})(i\mathbf{q})e^{i\mathbf{q}\cdot\mathbf{x}}\right]\right\rangle$$

$$= \exp\left[\frac{1}{2}\left\langle \left(\int d^2 q h(\mathbf{q})(\mathbf{k}\cdot\mathbf{q})e^{i\mathbf{q}\cdot\mathbf{x}}\right)^2\right\rangle\right]$$

$$= \exp\left[-\frac{1}{4}k^2\int d^2 q\, q^2 C(q)\right].$$

If we denote

$$\alpha = \int d^2 q\, q^2 C(q),$$

then

$$\langle[1+(\nabla h)^2]^{1/2}\rangle = \frac{1}{(2\pi)^2}\int d^2 w\int d^2 k e^{i\mathbf{k}\cdot\mathbf{w}}$$

$$\times \exp\left(-\frac{1}{4}\alpha k^2\right)(1+w^2)^{1/2}$$

$$= \frac{1}{\pi\alpha}\int d^2 w(1+w^2)^{1/2}e^{-w^2/\alpha}$$

$$= \frac{2}{\alpha}\int_0^\infty dw\, w(1+w^2)^{1/2}e^{-w^2/\alpha}. \quad (B1)$$

If we write $x=w^2/\alpha$, Eq. (B1) gives

$$\langle[1+(\nabla h)^2]^{1/2}\rangle = \int_0^\infty dx(1+\alpha x)^{1/2}e^{-x}.$$

For a self-affine fractal surface we have (see Sec. III) $\alpha = (q_0 h_0)^2 g(H)$ and denoting $\xi = q_0 h_0 g^{1/2}$ gives

$$\frac{\Delta\gamma_{\text{eff}}}{\Delta\gamma} = \int_0^\infty dx(1+\xi^2 x)^{1/2}e^{-x} - \frac{E}{2E_c}\xi^2. \quad (B2)$$

To quadratic order in ξ, the formulas (B2) and (14b) give the same result. In the limit $E/E_c \ll 1$, only $\xi \gg 1$ is of interest, and Eq. (B2) reduces to

$$\frac{\Delta\gamma_{\text{eff}}}{\Delta\gamma} \approx \xi\int_0^\infty dx\, x^{1/2}e^{-x} - \frac{E}{2E_c}\xi^2$$

$$= \left(\frac{\pi}{4}\right)^{1/2}\xi - \frac{E}{2E_c}\xi^2 \quad (B3)$$

to be compared with

$$\frac{\Delta\gamma_{\text{eff}}}{\Delta\gamma} \approx \xi - \frac{E}{2E_c}\xi^2 \quad (B4)$$

as obtained (in the limit $\xi \gg 1$) from the approximate formula (14b). From Eq. (B3), $\Delta\gamma_{\text{eff}}/\Delta\gamma$ is maximal for

$$q_0 h_c = \left(\frac{\pi}{4}\right)^{1/2}g^{-1/2}\frac{E_c}{E} \approx 0.89 g^{-1/2}\frac{E_c}{E}$$

and

$$(\Delta\gamma_{\text{eff}})_{\max} = \frac{\pi}{8}\frac{E_c}{E}\Delta\gamma \approx 0.39\frac{E_c}{E}\Delta\gamma.$$

The prefactors 0.89 and 0.39 in the exact theory should be compared with the prediction 1 and 0.5, which follows from the simpler theory [Eqs. (14b) and (B4)].

[1] B. N. J. Persson, *Sliding Friction: Physical Principles and Applications*, 2nd ed. (Springer, Heidelberg, 2000).
[2] B. N. J. Persson, J. Chem. Phys. **115**, 3840 (2001).
[3] K. N. G. Fuller and D. Tabor, Proc. R. Soc. London, Ser. A **345**, 327 (1975).
[4] K. L. Johnson, K. Kendall, and A. D. Roberts, Proc. R. Soc. London, Ser. A **324**, 301 (1971).
[5] B. N. J. Persson and R. Ryberg, Phys. Rev. B **32**, 3586 (1985); B. N. J. Persson, *ibid.* **63**, 104101 (2001).
[6] J. Feder, *Fractals* (Plenum, New York, 1988).
[7] M. Klüppel and G. Heinrich, Rubber Chem. Technol. **73**, 578 (2000).
[8] M. V. Berry and Z. V. Lewis, Proc. R. Soc. London, Ser. A **370**, 459 (1980).
[9] T. R. Thomas, *Rough Surfaces*, 2nd ed. (Imperial College Press, London, 1999).
[10] A. Chiche, P. Pareige, and C. Creton, C. R. Acad. Sci., Ser. IV **2000**, 1197.
[11] B. N. J. Persson, J. Chem. Phys. (in press).
[12] G. A. D. Briggs and B. J. Briscoe, J. Phys. D **10**, 2453 (1977).
[13] K. N. G. Fuller and A. D. Roberts, J. Phys. D **14**, 221 (1981).
[14] P. Tordjeman, E. Papon, and J-J. Villenave, J. Chem. Phys. **113**, 10712 (2000); C. Gay and L. Leibler, Phys. Rev. Lett. **82**, 936 (1999); A. Zosel, J. Adhes. **34**, 201 (1991); I. Chikina and C. Gay, Phys. Rev. Lett. **85**, 4546 (2000); C. Gay and L. Leibler, Phys. Today Nov. 1999, p. 48.
[15] See, e.g., L. B. Freund, *Dynamics Fracture Mechanics* (Cambridge University Press, New York, 1990).
[16] G. Sperling, Ph.D. thesis, Karlsruhe Technical University, 1964.
[17] K. Kendall, J. Phys. D **4**, 1186 (1971); **6**, 1782 (1973); **8**, 115 (1975). See also the beautiful review article of K. Kendall, Contemp. Phys. **21**, 277 (1980).
[18] B. N. J. Persson (unpublished).
[19] A. N. Gent and R. P. Petrich, Proc. R. Soc. London, Ser. A **310**, 433 (1969); M. Barquins, B. Khandani, and D. Maugis, C. R. Acad. Sci., Ser. II: Mec., Phys., Chim., Sci. Terre Univers. **303**, 1517 (1986); C. Derail, A. Allal, G. Marin, and Ph. Tordjeman, J. Adhes. **61**, 123 (1997); L. Benyahia, C. Verdier, and J.-M. Piau, *ibid.* **62**, 45 (1997).
[20] The decomposition of the roughness profile into "macroasperities" and shorter wavelength roughness is, of course, not unique. A rigorous treatment should be built on the formalism presented in Sec. III but with the inclusion of detachments.
[21] J. A. Greenwood, in *Fundamentals of Friction, Macroscopic and Microscopic Processes*, edited by I. L. Singer and H. M. Pollack (Kluwer, Dordrecht, 1992). See also, J. A. Greenwood and J. B. P. Williamson, Proc. R. Soc. London, Ser. A **295**, 300 (1966); J. F. Archard, *ibid.* **243**, 190 (1957); K. L. Johnson, *Contact Mechanics* (Cambridge University Press, Cambridge, 1985).
[22] The argument that thin glue layers give a stronger bond is only valid if the crack process zone is smaller than the thickness of the glue film. If this condition is not valid, thicker films may give the optimum adhesion. In practice glue layers below 15–20 μm are seldom used (C. Creton, private communication).
[23] H. Lakrout, P. Sergot, and C. Creton, J. Adhes. **69**, 307 (1999).
[24] A. N. Gent and C. Wang, J. Mater. Sci. **26**, 3392 (1991); A. N. Gent, Rubber Chem. Technol. **67**, 549 (1994).
[25] Y. L. Chen and J. Israelachvili, Science **252**, 1157 (1991).
[26] K. L. Johnson, *Contact Mechanics* (Cambridge University Press, Cambridge, 1985).